Subharmonic Excitation of the Shear Layer Between Two Ribs: Vortex Interaction and Pressure Field

S. Acharya,* T. A. Myrum,† and S. Inamdar‡
Louisiana State University, Baton Rouge, Louisiana 70803

An experimental study has been undertaken to examine the effect of subharmonic forcing on a curved, reattaching shear layer behind a rib in a ribbed-duct flow. With first subharmonic forcing, the vortex formation in the shear layer becomes regularized, but no pairing occurs. When the flow is forced at the second subharmonic, two vortices pair prior to reattachment. The pairing is accompanied by significant entrainment and shear-layer growth, which, in turn, leads to a dramatic reduction in the reattachment length. Three vortices appear to merge prior to reattachment when the external forcing is a third subharmonic of the most amplified frequency in the flow. The merging process is observed to be strong, and again leads to significant enhancements in entrainment. Phase-averaged pressures are shown to be related to the passage of vortices with the pressure above a pressure tap decreasing as the vortex or vortex pair passes by it and the pressure increasing as the vortices straddle the tap. The pressure spectra indicate that the initial vortex dynamics dictate the pressure field, with the response frequency, for all forcing frequencies and streamwise locations, being the measured natural frequency prior to pairing.

Introduction

THE existence of large-scale coherent structures in a turbulent shear layer and their dominant role in the entrainment, mixing, and other associated hydrodynamical processes is well established.[1-6] Moreover, the coherent structures in a mixing layer or a jet (classified herein as "simple" shear flows) can be manipulated with controlled excitation to promote vortex pairing and therefore turbulent mixing and shear-layer growth (see for example, Ref. 3). This fact, has great potential in improving the performance of many practical systems. For example, in gas turbine and other combustors, in internally ribbed heat exchangers, and in electronic cooling applications, the vigorous mixing between the core flow and the near-wall recirculating flow across the separated shear layer is critical. In many other aerospace-related applications, shear layers between a freestream and a recirculating flow are encountered (such as in stores attached to the fuselage). In all of these applications, if greater vortex pairing, and therefore mixing, could be obtained through controlled excitation, the resulting potential benefits could be significant.

Most studies on excited shear layers have been performed on "simple" shear layers (mixing layers or jets) where the shear layer is bounded on either side by well-defined freestream conditions. However, in many of the practical situations noted above, shear layers are more complex, and the shear layer is formed between a potential core subjected to a pressure gradient and a recirculating corner flow. Unlike "simple" shear layers, conditions on either side of the just mentioned "complex" shear layers vary with streamwise distance: the shear layer has streamline curvature and reattaches on a surface some distance downstream of separation. For this class of "complex" shear layers, studies dealing with the effect of controlled excitation, and more specifically subharmonic excitation, are very few, and therefore, this is the primary focus of the present paper.

The specific flow situation considered is flow in a pipe with two axisymmetric ribs (Fig. 1). The geometrical parameter values of primary interest in this paper are a rib-height-to-pipe-diameter ratio (e/D) of 0.36, and a rib-pitch-to-rib-height-ratio (P/e) of 7.1. For these values, the unforced flow generally does not reattach before the downstream rib. However, in view of the flapping nature of the shear layer, it may occasionally reattach in the interrib space.

The basic flow in this paper represents a curved separated shear layer, and thus resembles, in its overall structure, the separated flow past a backward facing step or a rib. Eaton and Johnston[7] have reviewed the earlier literature for flow past steps. Aung[8] and Baughn et al.[9] have reviewed both the hydrodynamic and heat transfer studies dealing with flow past steps, expansions, and cavities. Flow and heat transfer studies past ribs in a duct have been recently surveyed by Lau et al.[10]

As mentioned earlier, the literature dealing with the effect of excitation on reattaching separated shear layers between two ribs is very limited. In fact, the studies reported deal either with excited flows of a nonreattaching shear layer in a periodically fully developed ribbed channel flow[11-14] or excited flows over a backward facing step.[15-18] A reattaching forced shear layer between two ribs has not been heretofore considered. The primary objective of the present work is to correlate the external forcing with the observed vortex formation and pairing and to relate the coherent structure dynamics to the measured pressure fields. To this end, a special clocking mechanism is devised which permits the comparison of the forcing function, the flow visualization, and the measured pressures on the same time scale, and thus allows for a direct understanding of the pairing of large-scale structures and its effect on the pressure fields.

To summarize briefly the findings in the reported literature dealing with forced separated duct flows, Ghaddar et al.[11-13] and Patera and Mikic[14] have numerically solved the periodically fully developed duct flow subjected to infinitesimal disturbances. With oscillatory perturbation at the most unstable frequency, resonant excitation and associated transport enhancement are observed. In Refs. 15 and 16, the effect of the acoustic excitation of a laminar boundary-layer flow separating from a backward facing step has been examined. A premature transition to turbulence was observed, especially when the excitation frequency matched that of the naturally excited fluctuations in the shear layer. The reattachment length[17,18] for a separated flow over a backward facing step was reduced, due to vortex coalescence, for a certain range of excitation frequencies.

Received July 25, 1990; revision received Feb. 28, 1991; accepted for publication March 6, 1991.

*Professor, Mechanical Engineering Department.
†Assistant Professor, Mechanical Engineering Department.
‡Graduate Student, Mechanical Engineering Department.

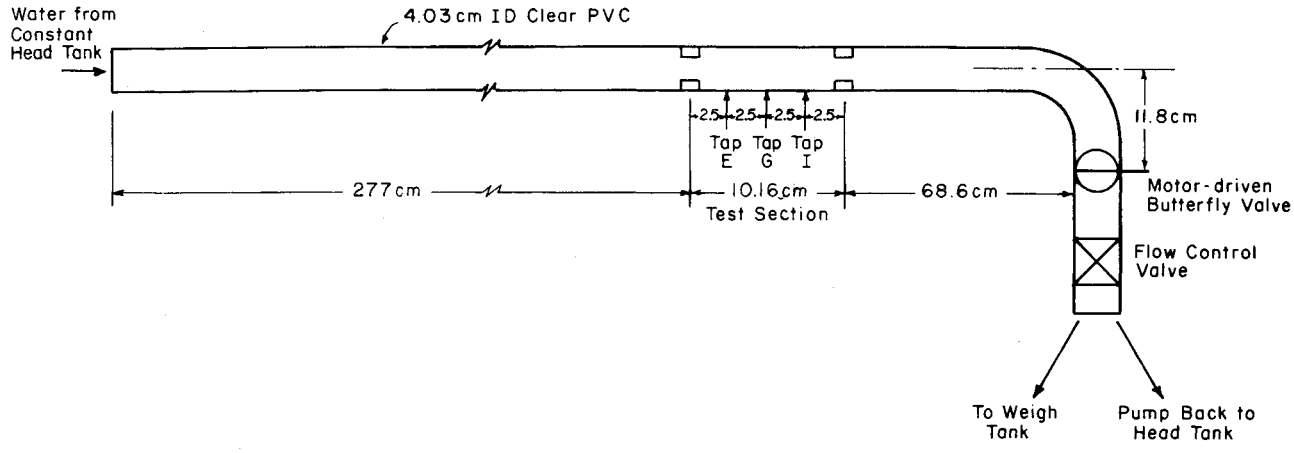

Fig. 1 Schematic of the experimental setup.

The specific objective of this paper is to examine the role of subharmonic forcing on the vortex pairing and pressure field in a separated shear layer between two axisymmetric ribs. Forcing at the fundamental, the first, second, and third subharmonic frequencies is studied. To limit the range of parameters, the effect of varying the amplitude of the forcing frequency is not studied in this paper. Of particular importance in this paper are flow visualization studies to understand the pairing of coherent structures at different subharmonic forcing frequencies and the correlation of the visualized structures with the measured data.

Experimental Setup

Figure 1 shows that water is delivered from a constant-head tank to the test section using a 4.03-cm-ID, 277-cm-long, clear PVC pipe. A butterfly valve located downstream of the test-section exit is used to excite the flow by alternately turning on and off the flow. The valve turns the flow on and off twice per revolution, thus one valve revolution corresponds to two complete pulsation cycles. The valve is controlled to provide excitation frequencies to within $\pm 2\%$ of their set-point values using a variable speed motor. All of the experiments were performed at an upstream, unpulsed Reynolds number (based on the pipe ID) of 1200 ($\pm 4\%$).

Wall pressure information was obtained using a Scanivalve PDCR23D differential pressure transducer with a worst-case static pressure accuracy of ± 0.015 psid and a sensitivity of 5 psid/V. The pressure was conveyed to the transducer using a 1.59-mm-ID, 25-cm-long flexible tube that was attached to various 0.079-cm-ID brass tubes that were mounted flush with the inside wall of the test section. For the same flexible tubing (i.e., material, ID, and length), Scanivalve reports, for 99.9% stabilization, a frequency response of 62 Hz, 10 times the unforced vortex shedding frequency. The response was for air-filled tubing and represents a lower bound, since the tubes were completely filled with water for all of the experiments.

The pressure signals were recorded at 100 times the excitation frequency using a Metrabyte EXP-16 A/D board. The maximum uncertainty was less than $\pm 2\%$ of the minimum recorded pressure. In order to correlate the instantaneous pressure with the instantaneous valve position and to facilitate the phase averaging of the pressure signal, the sampling was initiated by externally triggering the A/D board when the valve was in the fully closed position.

Phase-averaged pressures were obtained for one complete valve revolution. Note that this corresponds to two pulsation cycles. The phase averaging consisted of arithmetically averaging the instantaneous pressures at a common valve position for a number of cycles. This was repeated for all of the 200 valve positions comprising a single revolution.

Visualization of the shear layer was accomplished by metering a mixture of water and ordinary food coloring into the flow at the surfce of the upstream rib. The flow patterns were recorded in the VHS mode at 30 frames per second using a Sony M7 Professional Television Camera with 700 lines of resolution. Each frame contained two fields. Therefore, the camera was actually capable of capturing 60 individual events per second.

In order to synchronize the instantaneous wall pressures with the instantaneous flow behavior and to correlate the instantaneous valve position with the instantaneous flowfield, an electronic signal, which showed up as an audible click on the audio track of the VHS tape, was conveyed to the camera when the pulsing valve was in the fully closed position. Recall, this is the precise instant of time at which the A/D board is triggered, so the pressure corresponding to the valve closure represents the first pressure reading of the forcing period. Therefore, the flow visualization pictures can be directly linked to the instantaneous pressure.

Results and Discussion

In properly interpreting the results described below, it should be noted that while the forcing frequency f_f is externally introduced into the flow, it could be accompanied by the presence of additional frequencies arising out of waterhammer and the impingement of the flow on the second rib. However, the amplitude of the forcing frequency is believed to be considerably higher than those of the additional frequencies. The effect of forcing simultaneously at the fundamental and the subharmonic has been studied.[19-22] In these studies, as for pure subharmonic forcing, enhanced vortex pairing and shear-layer growth is observed, but the phase relation between the fundamental and subharmonic now controls the amplification rate. However, the above studies were for cases where both frequencies are introduced at the same amplitude. In the present case, the dominating amplitude is at a single forcing frequency, equal to the fundamental or a subharmonic value. The additional weaker frequencies, if not at the fundamental or subharmonic, are not likely to be amplified.

Flow Patterns

Figure 2a shows the typical shear layer that forms for an unforced flow past a rib. It is seen that the flow does not reattach the interrib space. Note that the dye streak appears as a fine coherent ribbon, which persists for about 1.5 rib heights with no diffusion. This fact, coupled with the relatively low flow velocity (Re = 1200) suggests a laminar flow structure.

Using a strobelight, the natural, unforced vortex shedding frequency, f_o, of this flow was measured to within $\pm 10\%$ and was found to be 6.2 Hz. This was confirmed later using the

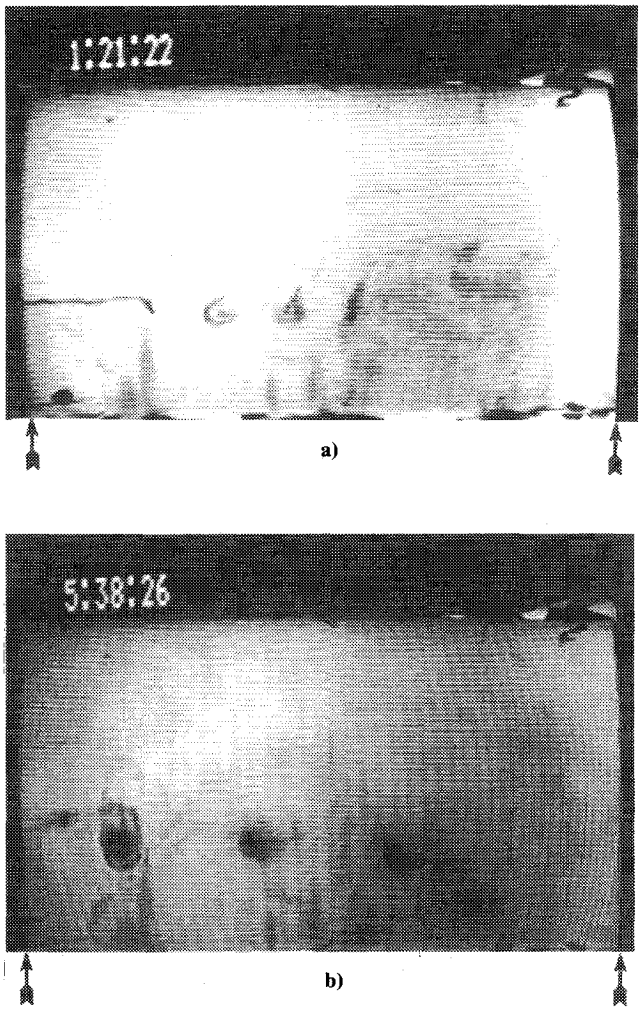

Fig. 2 Flow visualization pictures: a) unforced; b) first subharmonic forcing, f_f = 6.3 Hz. Arrows denote rib location.

"clock" on the VHS tape. Based on the camera's ability to capture 60 events per second, the uncertainty at 6.2 Hz is ±10%.

The photograph in Fig. 2b demonstrates the effect of forcing the shear layer at a forcing frequency of f_f = 6.3 Hz, i.e., about the same frequency as the natural, unforced frequency f_o. Unlike the unforced shear layer, the forced shear layer reattaches in the interrib space between 4.8 and 5.7 rib heights. Using the "clock," it was found that the vortex passage frequency matched that of the forcing frequency. Ho and Huang[3] found that the vortex passage frequency in a mixing layer flow was the dominant frequency and termed this frequency the response frequency. They also observed that the response frequency matched the forcing frequency when the mixing layer was pulsed at the natural, unforced frequency in the mixing layer.

Figures 3a–d show the response of the shear layer to a forcing frequency of 3.3 Hz (i.e., about one-half the unforced frequency) at different instants of time. The most distinguishing feature is the merging of the two vortices and subsequent downstream convection of the newly formed structure (Fig. 3d). Ho and Huang[3] also observed the merging of two vortices at a fixed location for mixing layers when the forcing frequency is one-half the natural frequency of the layer. When the initial boundary layer was laminar, Zaman and Hussain[4] and Kibens[23] observed the same type of pairing as seen in Fig. 3b for the controlled excitation of a circular jet. They referred to this type merging as "shear-layer mode pairing" (characterized by the two vortices deforming with a near-S shape demarcation line between the vortices prior to merging). Recall that the flow visualization in this study indicates laminar flow conditions near the rib surface. It should be mentioned that even for large excitation amplitudes and turbulent exit conditions, Fielder and Mensing[24] have observed shear-layer mode pairing.

The vortex pairing occurred at about 2 rib heights, and significant spreading (see Fig. 3b) around the merging location resulting from the lateral displacement of the vortices was observed. Consequently, the reattachment length is reduced from that (5 to 6 rib heights) for the 6.3-Hz case to about 3 to 4 rib heights. The vortex passage frequency was found to be 6.0 Hz (±10%), i.e., about 2 times the forcing frequency, upstream of the pairing location. This was also observed in Ref. 3 for mixing layers. Downstream of the pairing location the frequency was 3.3 Hz (±5%), close to the forcing frequency.

Figures 4a–d correspond to a 2.0-Hz forcing frequency ($\approx 1/3\, f_o$). Figure 4a shows two independent structures, while Figs. 4b and 4c show these structures merging together to form one structure. Suggestive of "shear-layer mode"[4] pairing, the leading vortex moves toward the wall prior to merging (Fig. 4b). During the merging of the first two vortices, a third vortex appears (Figs. 4a and 4d). This vortex is the most energetic one, and as seen in Figs. 4c and 4d, it accelerates toward the first two votices. The third vortex appears to merge explosively with the paired structure in Fig. 4d, but because of the tremendous spreading of the structure formed by the first two vortices, it was not possible to determine if complete merging actually occurs.

Because of the large spreading rate, the reattachment length for the 2.0-Hz case was less than that for the 3.3-Hz case, with reattachment occurring between 2 and 4 rib heights. The initial vortex passage frequency was estimated at 6.0 Hz (±10%), three times the forcing frequency.

Vortex Trajectories and Velocities

Vortex trajectories and convection velocities are plotted in Figs. 5 and 6 for f_f/f_o = 0.5 (3.3-Hz case) and f_f/f_o = 0.3 (2.0-Hz case), respectively. In the figures, x is the streamwise distance between the first rib and the vortex center, y is the cross-stream displacement between the tube wall and the vortex center, e (= 1.4 cm) is the rib height, v_x is the streamwise vortex convection velocity, and v_{av} (= 0.36 m/s) is the average, unpulsed rib-jet velocity (i.e., the average velocity through the ring which forms the rib).

The x and y distances were measured using a grid with a 0.2-cm resolution, superimposed on the tube, while the velocities were determined by dividing the change in the x position of the vortex by the corresponding time change (time intervals were either 0.033 or 0.017 s as measured by the "clock" on the VHS tape). In this arrangement, the change in x varied between 0.3 to 1.3 cm.

The data points on the figures represent the measured x, y, and v_x values. These values were phase averaged over 10 different cycles. Although considerable effort went into ensuring the accuracy of the data in Figs. 5 and 6, the purpose of the figures is to present qualitative insights into the vortex merging process rather than quantitative velocity and position measurements.

Figure 5a shows that for f_f/f_o = 0.5, vortex 1 is initially above the upper surface of the rib where it is influenced by the jetlike flow through the ID of the rib. As it convects downstream, it moves downward, behind the rib where the velocities are relatively low. Consequently, the velocity decreases (see Fig. 5b) until both the velocity and displacement attain their minimum values at about x/e = 2.

Vortex 2 is shed when vortex 1 is at about x/e = 1.3. It moves out into the jet-like flow as it convects downstream. Consequently, there is a sharp increase in the convective velocity. This enables vortex 2 to catch up and subsequently merge with vortex 1 via kinematic induction (see Figs. 3a–d).

In the foregoing, the merging of the vortices is attributed to the fact that the difference in the convective velocities of

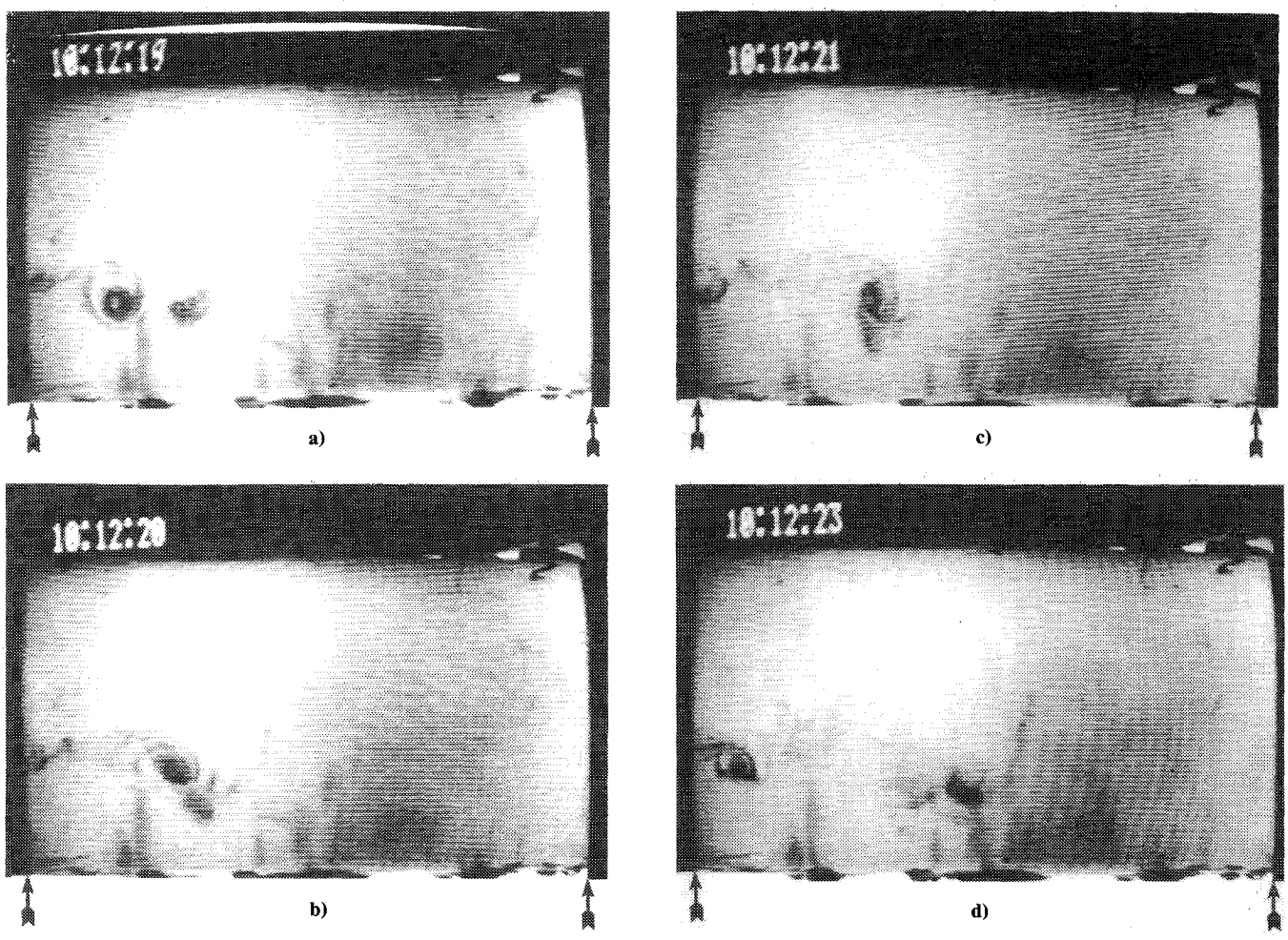

Fig. 3 Flow visualization pictures for second subharmonic forcing, f_f = 3.3 Hz: a–d) pictures taken at several time instances as indicated by the clock in the upper left corner of each picture. Arrows denote rib location.

the respective vortices enables vortex 2 to catch up with vortex 1. This, in turn, is related to the lateral displacement of the individual vortices as they moved downstream. Ho and Huang[3] used the same reasoning to explain the merging of M vortices in an excited mixing layer flow. When the layer is forced at the Mth subharmonic of the response frequency, the energy supplied at the Mth subharmonic is amplified downstream by the shear layer instability. This causes M vortices to be displaced to different lateral locations according to the individual phase differences between the vortices and the subharmonic. In the present case, the response frequency is 6.0 Hz, and the forcing frequency is 3.3 Hz. Therefore, the lateral displacement of two vortices is occurring when the forcing frequency is the second subharmonic of the response frequency and the explanation in Ref. 3 seems to apply to the f_f/f_o = 0.5 case.

Figure 6a shows for f_f/f_o = 0.3 that vortex 1 (the leading vortex) moves toward the tube wall as it convects downstream. Consequently, its velocity decreases. When vortex 1 is at about x/e = 1.3, vortex 2 is shed. As vortex 2 convects downstream, its velocity is independent of x/e. This is because vortex 2 is initially displaced into the jetlike flow, which dominates its behavior up to about x/e = 1.5. Beyond this point, vortex 2 moves toward the wall and eventually merges with vortex 1 at about x/e = 2.4. After merging, the velocity of the resulting structure decreases as it convects downstream. This is because the structure dilates considerably (see Figs. 4c and 4d) as it moves downstream, causing the lower extremities of the structure to interact with the tube wall. Vortex 3 is shed shortly before the paired structure reaches the final x/e value displayed in Fig. 6a. It is seen that the trajectory of vortex 3 is virtually uniform. Figure 6b shows that initially the velocity is around 50% of the average rib jet velocity and that this velocity increases sharply to a maximum value which is 10% above the average rib jet velocity. Subsequently, the velocity decays slightly between x/e = 1.5 and 2.3.

The displacement between the symbol for paired structure and that for vortex 3 near x/e = 2.7 represents the distance between the approximate centers. Recall the paired structure dilates considerably after pairing.

Phase-Averaged Pressure Distributions

The phase-averaged pressure distributions (Figs. 7, 9, and 11) together with schematics of the corresponding instantaneous flow structure (Figs. 8, 10, and 12) during one flow cycle now will be considered in order to directly correlate the observed flow structure with the measured pressures. Respectively, the pressure and time in Figs. 7, 9, and 11 have been nondimensionalized by the pressure head (P_{st} = 27.5 kPa) for no flow and the forcing period ($T_c = 1/f_f$). Since in a reattaching shear layer, the initial stages of vortex formation and pairing are critical, attention is primarily focused on tap E, which is 1.83 cm downstream of the rib.

In the absence of external forcing, the pressures measured by the transducer do not exhibit large variations. The vortices are small (Fig. 2a), entrainment rates are low, and there is significant temporal and spatial jitter in the evolution and pairing processes. The transducer used is not sensitive enough to accurately pick up the fluctuations associated with the unforced case, and no effort was made to separate out inaccuracies, say due to noise, from the true fluctuations. With subharmonic excitation, vortex formation becomes regular-

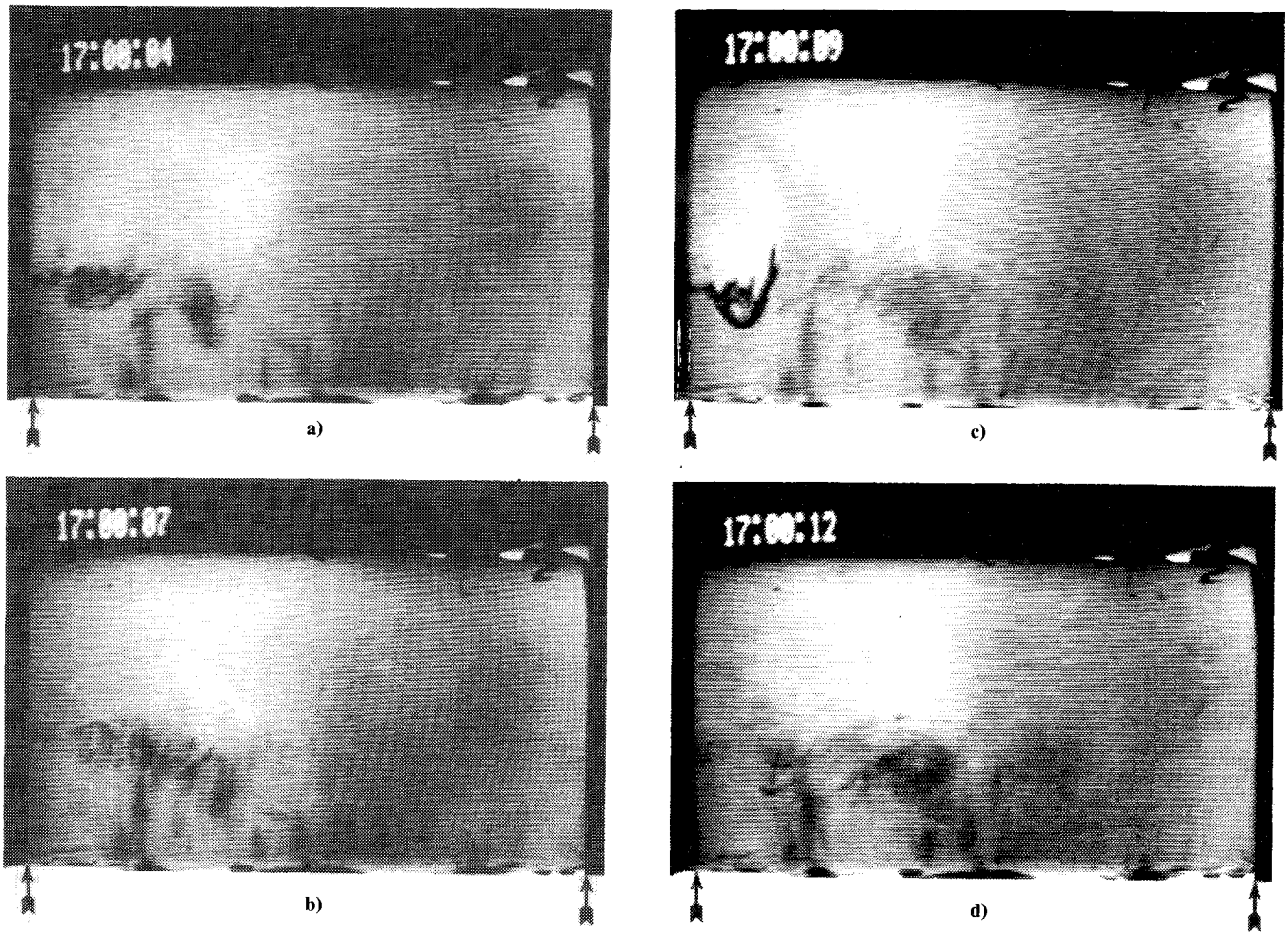

Fig. 4 Flow visualization pictures for third subharmonic forcing, f_f = 2.0 Hz: a–d) pictures taken at several time instances as indicated by the clock in the upper left corner of each picture. Arrows denote rib location.

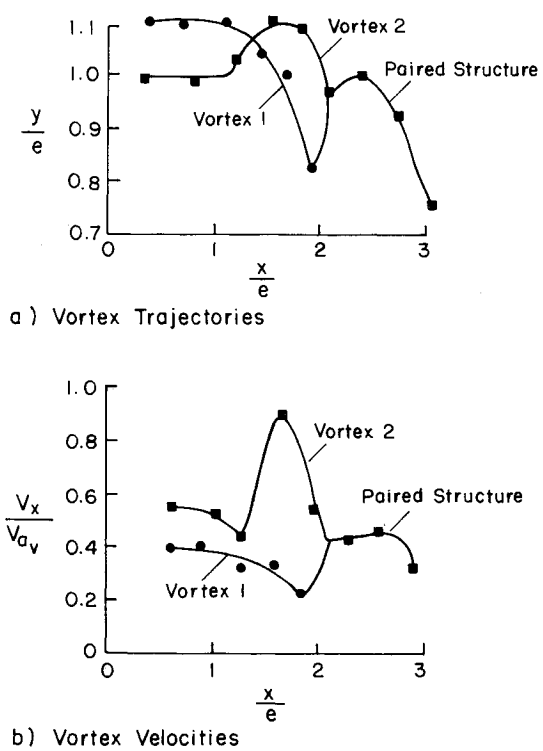

Fig. 5 Second subharmonic forcing.

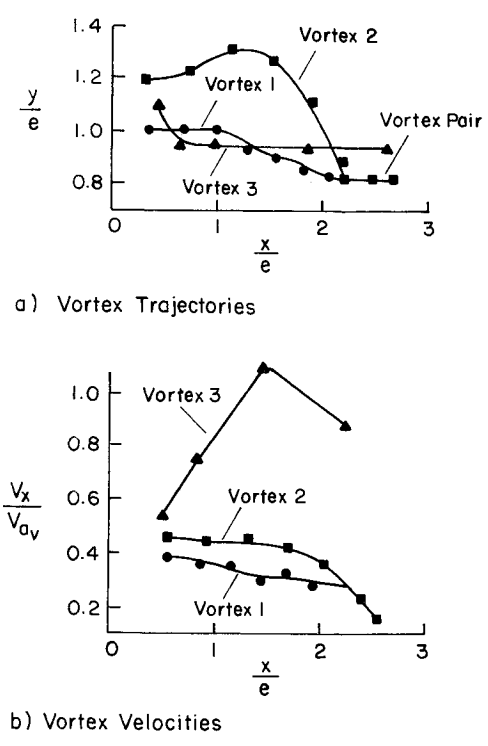

Fig. 6 Third subharmonic forcing.

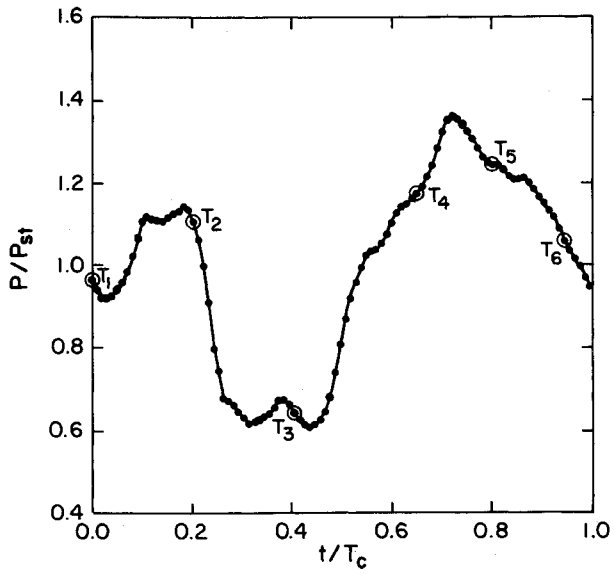

Fig. 7 Phase-averaged pressures for first subharmonic forcing (T_c = 0.16 s).

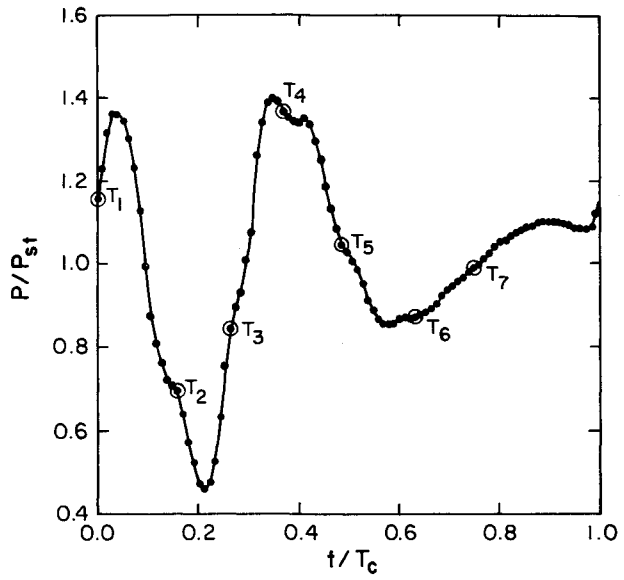

Fig. 9 Phase-averaged pressures for second subharmonic forcing (T_c = 0.30 s).

ized (Figs. 2b–4), pairing activity and entrainment is significantly enhanced, and the pressure variations are distinctly picked up.

For first subharmonic forcing, the vortex formation occurs at periodic and regular intervals (see Figs 2b and 8), and the pressure excursions in Fig. 7 are linked to the passage of the vortices (or pairs of vortices if pairing occurs as it does for other subharmonics). The flow patterns corresponding to the pressures in Fig. 7 are shown schematically in Fig. 8 at different instances of time, marked T_1 through T_6. This notation is also used in the pressure plots (Fig. 7) in order to link the flow structure to the pressure behavior.

As seen in Fig. 8, the shear layer structure is one of vortices or vortices in tandem connected by thin braids. Entrainment occurs as fluid is drawn along the braid and is rolled up into the vortex core. At T_1, the valve is fully closed, tap E is straddled on either side by vortices (termed vortex 1 and vortex 2), and the entrainment into the vortices is primarily from the high-speed side of the shear layer. Thus, in relative terms, there is no acceleration of the flow near tap E, and the pressure rises from T_1 to T_2. From time T_2 to T_3, vortex 1 entrains fluid along its braid, and the flow in the vicinity of tap E accelerates, causing the pressure to drop. As vortex 1 moves further downstream, the pressure rises again (from T_3 to T_4) until vortex 2 passes over tap E (at around T_5), and again the flow in the vicinity of tap E accelerates due to the passage of vortex 2. This causes the pressure to drop. At T_6, the valve is again nearing the fully closed position.

When the flow is forced at the second subharmonic (Figs. 9 and 10), two vortices merge, and due to the near-wall effects, only a single merging occurs. At T_1, the valve is fully closed; vortex 1 is entraining fluid primarily from the high-speed side (see Fig. 10), and as seen in Fig. 9, the pressure near the tap E begins to rise. At T_2, vortex 1 is in the vicinity of tap E, and the flow begins to accelerate as the vortex moves over the tap. At T_3, vortex 1 is immediately above the tap, and

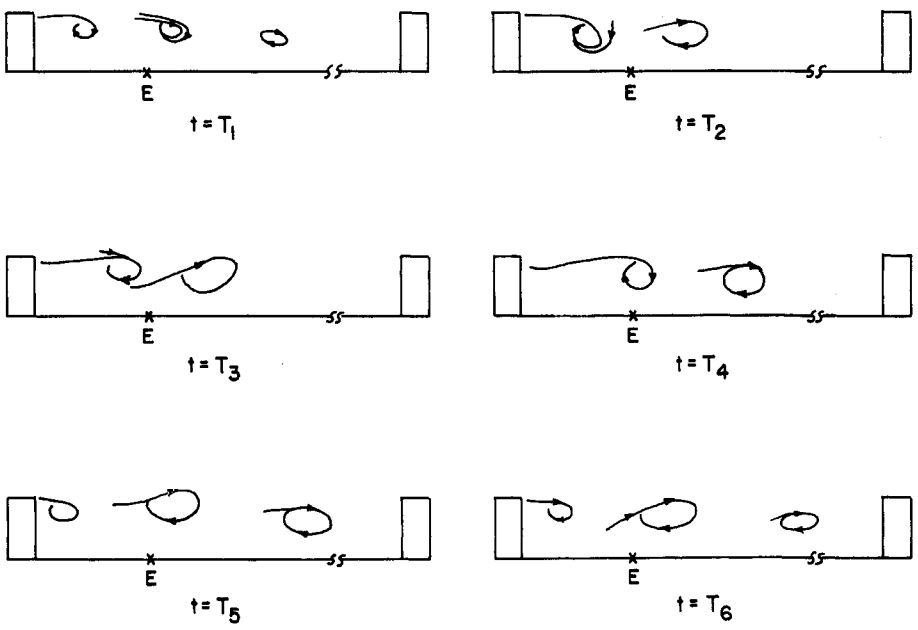

Fig. 8 Flow pattern schematic at several time instances for first subharmonic forcing.

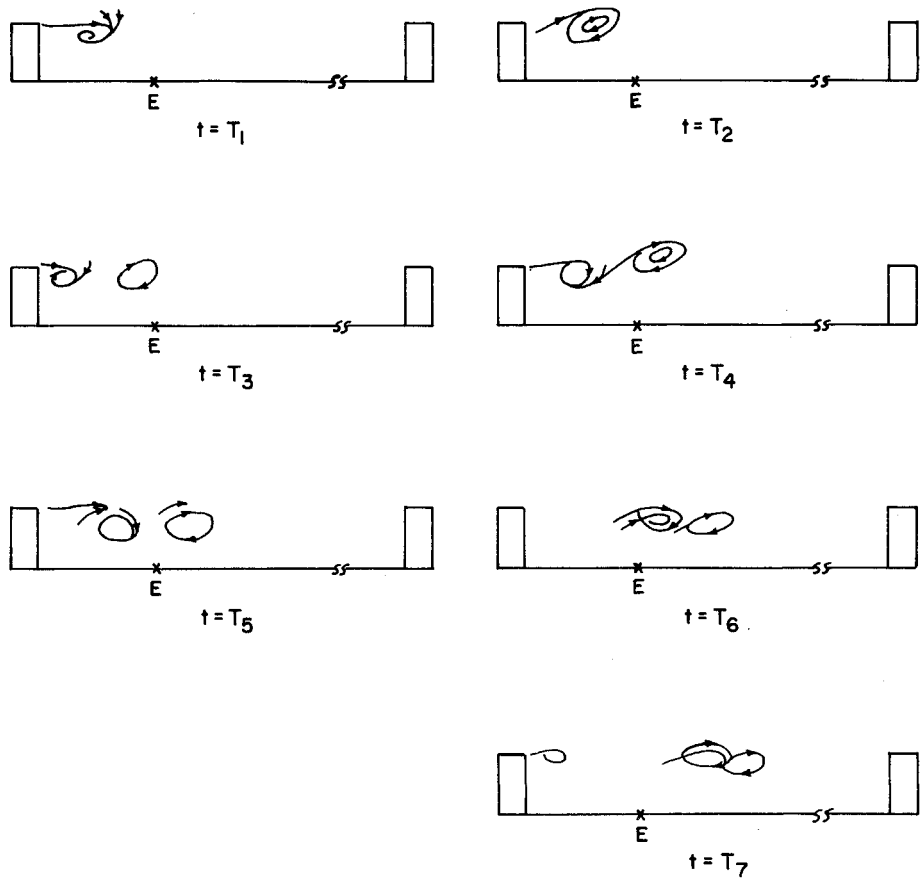

Fig. 10 Flow pattern schematic at several time instances for second subharmonic forcing.

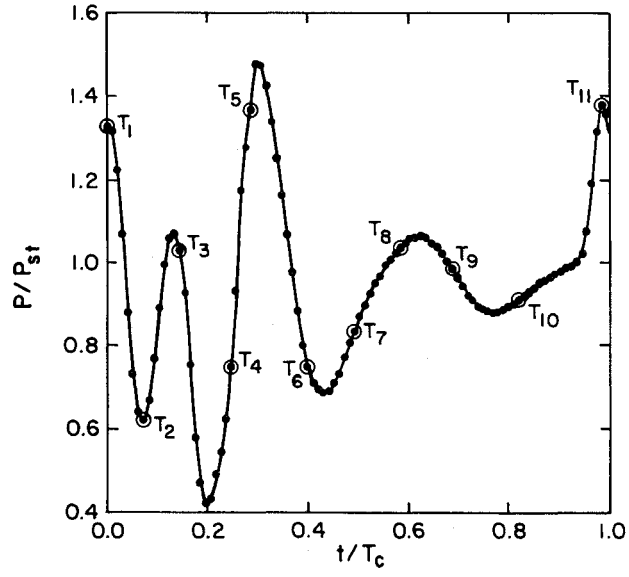

Fig. 11 Phase-averaged pressures for third subharmonic forcing (T_c = 0.50 s).

pressure has a local minimum between T_2 and T_3 due to the induced velocity. Simultaneously, vortex 2 forms behind the step. The vortices 1 and 2 straddle at tap E at T_4, and the pressure rises. Vortex 2 is approaching tap E at T_5, and between time T_5 and T_6, vortex 2 passes across tap E, causing the flow to accelerate. Consequently, the pressure in the vicinity of the tap decreases. The vortices are in the process of pairing at time T_7 and are slightly beyond the tap. A moderate increase in pressure is noted from T_6 to T_7 as the valve closes.

The flow, when forced at the third subharmonic, is observed to result in the merging of three vortices (Fig. 12). At the fully closed position T_1, vortex 1 is beyond tap E and vortex 2 is approaching it. Between T_1 and T_2, the flow acceleration caused by the entrainment from vortex 1 leads to a drop in pressure (Fig. 11). Between T_2 and T_3, vortex 1 and vortex 2 straddle tap E, and entrainment is primarily from the high-speed side. Consequently, the pressure increases. As vortex 2 moves past tap E, the flow is accelerated and the pressure drops between T_3 and T_4. At T_4, the third and most energetic vortex is also formed. Vortices 1 and 2 begin to pair at T_5, at which time, this quasipaired structure and vortex 3 straddle the pressure tap. The pressure, therefore, rises from T_4 to T_5. Vortex 3 crosses the tap at T_6, and accelerates the near-tap fluid, again causing the pressure to drop. Pairing between vortex 3 and the almost-paired vortices 1 and 2 begins around T_7. The paired vortices move downstream, the flow decelerates, and the pressure rises again from T_7 to T_8. At T_9, the above scenario begins again, and a new vortex 1 is formed. At T_{10}, the vortex passes by tap E, and the pressure attains a local minimum. At T_{11}, vortices 1 and 2 straddle tap E, as at T_1, and the pressure rises from that at T_{10} to that at T_{11}.

Pressure Spectra

The pressure spectra were calculated from 512 data points. This gives a worst-case resolution at the 620-Hz sampling frequency of ±0.61 Hz. By sampling the output of a sine wave generator, it was confirmed that fluctuations of up to 70 Hz could be detected at the minimum sampling frequency (157 Hz) used for the experiments.

The pressure spectra are shown in Figs. 13–16 for the four subharmonic forcing frequencies considered in this paper. At

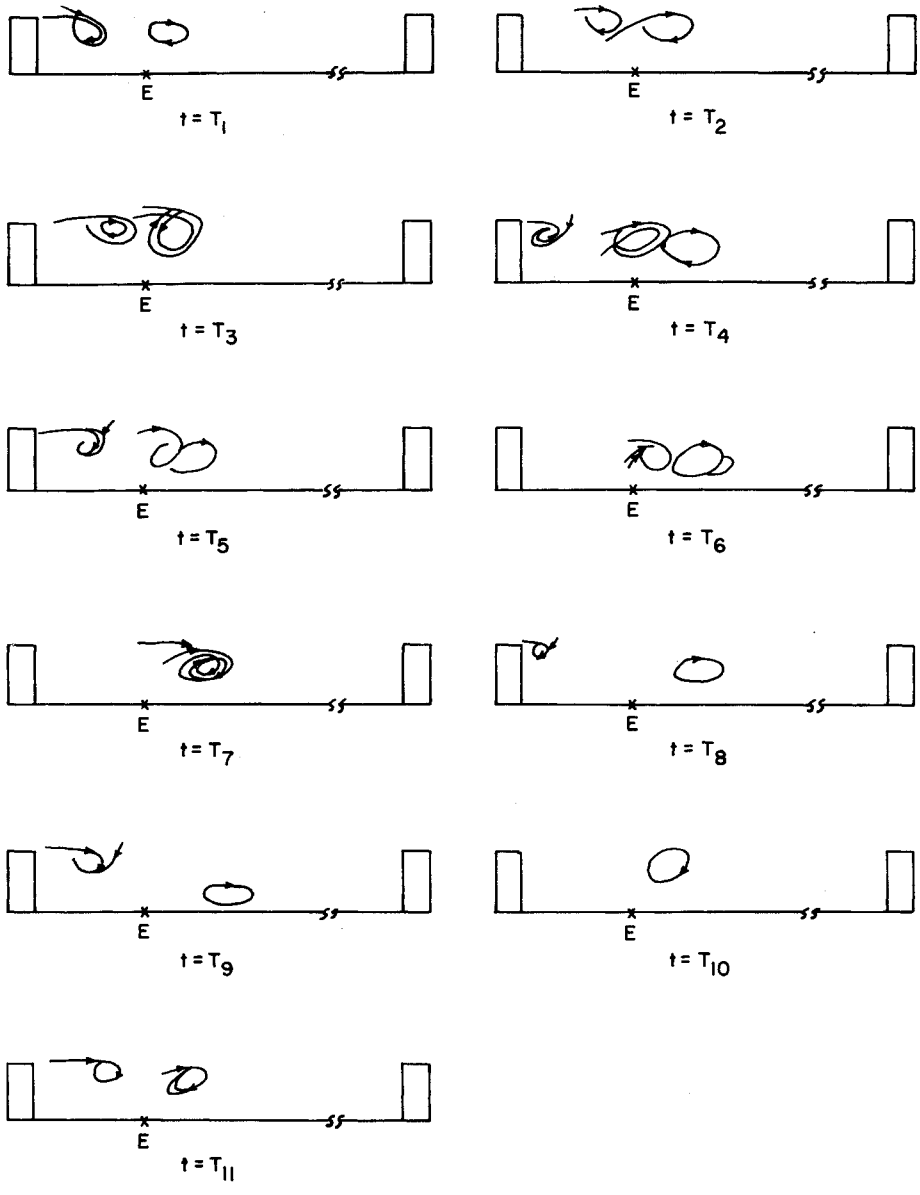

Fig. 12 Flow pattern schematic at several time instances for third subharmonic forcing.

each forcing frequency, the spectra at the three streamwise tap locations (denoted by E, G, and I in Fig. 1) are shown. Three major features are observed in the spectra profiles: 1) The response frequency, for all subharmonic forcing frequencies, appears to be the most probable frequency f_m measured for the unexcited flow situation. 2) Due to nonlinear amplification, higher harmonics of the forcing frequency f_f are always obtained. In particular, the harmonic frequency closest to f_m, and on the higher side, is always distinctly observed. 3) The entire streamwise distance is dominated by the initial coherent structure dynamics. Thus, the spectra at G and I are very similar to that obtained at E.

The first observation that the most probable frequency dominated the spectra at tap E is clearly understandable, since tap E is generally slightly upstream of vortex merging, and therefore any reduction in frequency expected due to vortex pairing is not observed. For second and third subharmonic forcing, the forcing frequencies do not manifest themselves strongly in the spectra. In these cases, the forcing frequency is sufficiently lower than f_m, which is the most probable amplified frequency. However, one of the higher harmonics of the forcing frequency is closer to f_m, and this frequency is preferentially amplified at a higher rate and becomes the dominant response frequency in the flow. Thus, regardless of the forcing frequency, a dominant or very strong peak is always obtained at f_m. Ho and Huang[3] have observed a similar behavior in their "simple" shear-layer studies.

Mode Diagram

A mode diagram (Fig. 17), similar to that of Ho and Huang,[3] can be plotted for the present results. The theoretical most amplified frequency f_m was taken to be the most probable vortex passage frequency f_o as measured under unforced conditions. There was some ambiguity in the reponse frequency f_r for certain cases, since, as noted above, the higher harmonic of the forcing frequency that is immediately larger than f_m is in some cases also strongly amplified with peaks comparable to or slightly greater than that at f_m. However, in such cases, the bandwidth of the spectrum around f_m is always larger, and this is probably due to the temporal and spatial jitters in the flow at this frequency. Keeping this in mind, the dominant response frequency f_r, from the perspective of both the peak and the bandwidth, is always f_m, and is taken as f_r, in the mode diagram plot in Fig. 17. The mode diagram plot is a straight line given by $f_r = f_m$, and the response frequency and the forcing frequency are related by the equation $f_r = Mf_f$, where M is 1 for the first subharmonic forcing frequency, 2 for the second subharmonic forcing frequency, and so on. Again, this observation seems to be consistent with those observed by Ho and Huang.[3]

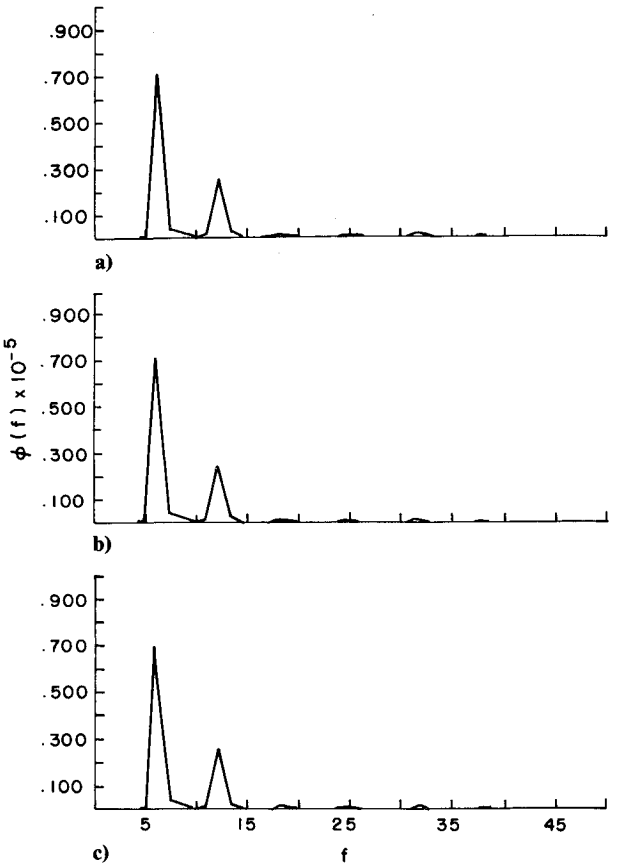

Fig. 13 Pressure spectra for first subharmonic forcing: a) tap E, $x/e = 2$; b) tap G, $x/e = 4$; and c) tap I, $x/e = 6$.

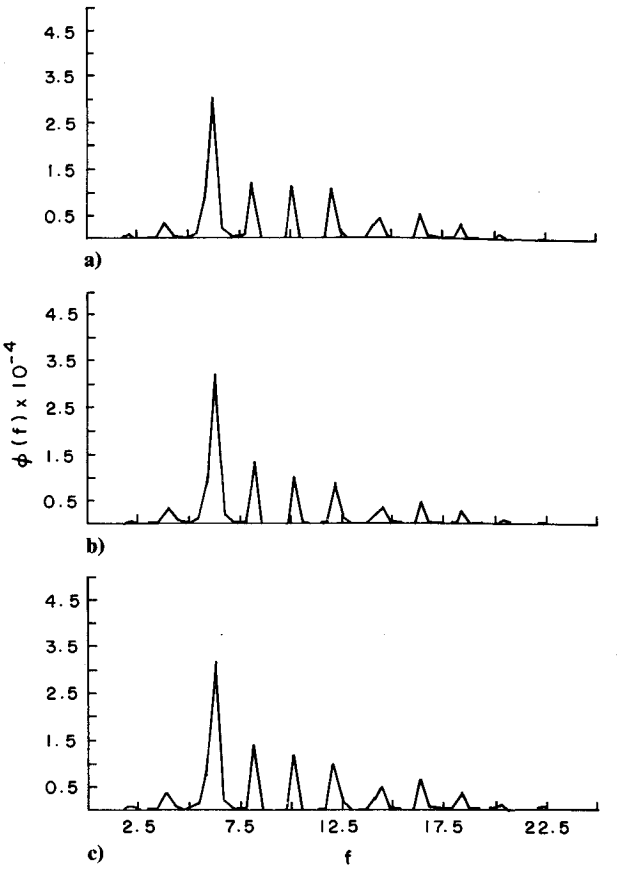

Fig. 15 Pressure spectra for third subharmonic forcing: a) tap E, $x/e = 2$; b) tap G, $x/e = 4$; and c) tap I, $x/e = 6$.

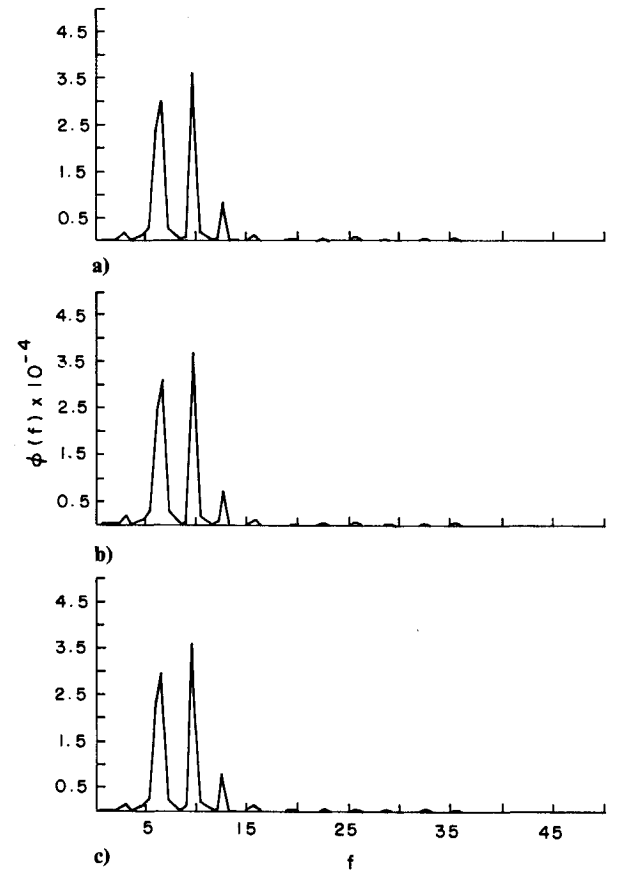

Fig. 14 Pressure spectra for second subharmonic forcing: a) tap E, $x/e = 2$; b) tap G, $x/e = 4$; and c) tap I, $x/e = 6$.

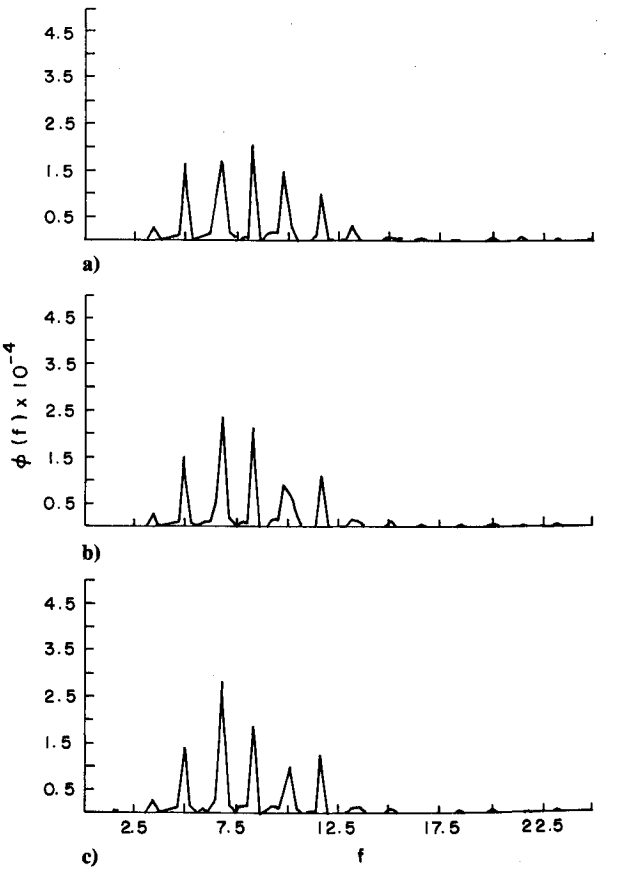

Fig. 16 Pressure spectra for fourth subharmonic forcing: a) tap E, $x/e = 2$; b) tap G, $x/e = 4$; and c) tap I, $x/e = 6$.

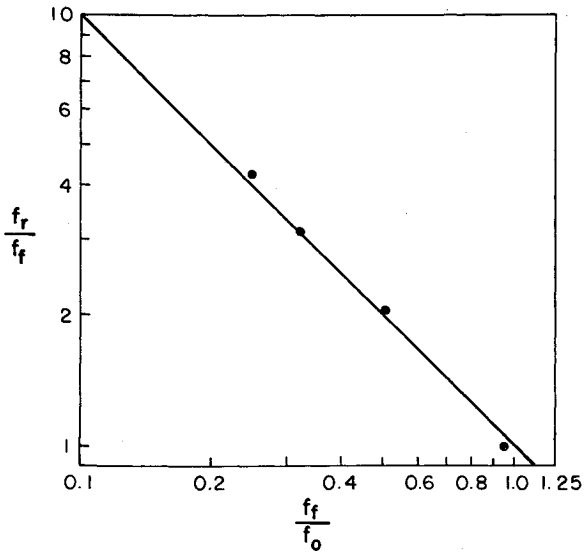

Fig. 17 Mode diagram.

Concluding Remarks

The following major conclusions can be reached from the results of this study.

1) As in "simple" shear layers, the subharmonic forcing of a "complex" reattaching, curved shear layer past a rib in a ribbed duct flow leads to vortex pairing, a significant increase in the entrainment, and a companion decrease in the reattachment length.

2) Forcing at the first subharmonic regularizes vortex formation, forcing at the second subharmonic leads to pairing of two vortices, and forcing at the third subharmonic leads to pairing of three vortices. Due to the presence of the wall, only a single pairing was observed prior to reattachment. The vortex merging behavior appears to be similar to that in "simple" shear layers, in that, forcing at the Mth subharmonic leads to the merging of M vortices.

3) Phase-averaged pressure variations have been shown to be directly linked to the passage of vortices or paired vortices past the measurement location. The near-field coherent structure dynamics appear to dominate the pressure field at all streamwise distances.

4) Regardless of the forcing frequency, the response frequency is always observed to be the most amplified frequency in the unforced flow. This is due to the preferential amplification of the higher harmonics of the forcing frequency.

Acknowledgments

This material is based upon work supported by the National Science Foundation under Grant No. CBT-8800736. The U.S. Government has certain rights in this material.

References

[1]Roshko, A., "Structure of Turbulent Shear Flows, A New Look," *AIAA Journal*, Vol. 14, 1976, pp. 1349–1357.

[2]Browand, F. K., and Laufer, J., "The Role of Large Scale Structures in the Initial Development of Circular Jets," *Turbulence in Liquids*, edited by J. L. Zakia and Z. K. Patterson, Princeton, NJ, 1975.

[3]Ho, C. M., Huang, L. S., "Subharmonic and Vortex Merging in Mixing Layers," *Journal of Fluid Mechanics*, Vol. 119, 1982, pp. 443–473.

[4]Zaman, K. B. M. Q., and Hussain, A. K. M. F., "Vortex Pairing in a Circular Jet Under Controlled Excitation: Part 1. General Jet Response," *Journal of Fluid Mechanics*, Vol. 101, 1980, pp. 449–491.

[5]Hussain, A. K. M. F., and Zaman, K. B. M. Q., "Vortex Pairing in a Circular Jet Under Controlled Excitation: Part II. Coherent Structure Dynamics," *Journal of Fluid Mechanics*, Vol. 101, 1980, pp. 493–547.

[6]Zaman, K. B. M. Q., "Farfield Noise of a Subsonic Jet Under Controlled Excitation," *Journal of Fluid Mechanics*, Vol. 152, 1985, pp. 83–111.

[7]Eaton, J. K., and Johnston, J. P., "A Review of Research on Subsonic Turbulent Flow Reattachment," *AIAA Journal*, Vol. 19, 1981, 1093–1100.

[8]Aung, W., "Separated Forced Convection," *Proceedings of the ASME-JSEM Thermal Engineering Conference*, Hawaii, 1983, pp. 499–515.

[9]Baughn, J. W., Hoffman, M. A., Launder, B. E., Lee, D., and Yap, C., "Heat Transfer, Temperature and Velocity Measurements Downstream of an Abrupt Expansion in a Circular Tube at a Uniform Wall Temperature," *Journal of Heat Transfer*, Vol. 111, 1989, pp. 870–876.

[10]Lau, S. C., McMillin, R. D., and Han, J. C., "Heat Transfer Characteristics of Turbulent Flow in a Square Channel with Angled Discrete Ribs," ASME 90-GT-254, Gas Turbine and Aeroengine Congress, Brussels, June 11–14, 1990.

[11]Ghaddar, N. K., Greiner, M., Patera, A. T., and Mikic, B. B., "Heat Transfer Enhancement by Oscillatory Perturbation of a Stable Separated Flow," *International Communications Heat Mass Transfer*, Vol. 12, 1985, pp. 369–379.

[12]Ghaddar, N. K., Korczak, K. Z., Mikic, B. B., and Patera, A. T., "Numerical Investigation of Incompressible Flow in Grooved Channels: Part I. Stability and Self-Sustained Oscillations," *Journal of Fluid Mechanics*, Vol. 163, 1986, pp. 99–127.

[13]Ghaddar, N. K., Magen, M., Mikic, B. B., and Patera, A. T., "Numerical Investigation of Incompressible Flow in Grooved Channels: Part II. Resonance and Oscillatory Heat Transfer Enhancement," *Journal of Fluid Mechanics*, Vol. 168, 1986, pp. 541–567.

[14]Patera, A. J., and Mikic, B. B., "Exploiting Hydrodynamic Instabilities: Resonant Heat Transfer Enhancement," *International Journal of Heat and Mass Transfer*, Vol. 29, 1986, pp. 1127–1138.

[15]Sato, H., "Experimental Investigation on the Transition of Two-Dimensional Separated Layer at Subsonic Speeds," *Journal of the Physical Society of Japan*, Vol. 11, 1956, pp. 702–709.

[16]Sato, H. "Further Investigation on the Transition of Two-Dimensional Separated Layer at Subsonic Speeds," *Journal of the Physical Society of Japan*, Vol. 14, 1959, pp. 1797–1810.

[17]Roos, F. W., and Kegelman, J. T., "Influence of Excitation on Coherent Structures in Reattaching Turbulent Shear Layers," AIAA Paper 86-0112, Jan. 1986.

[18]Bhattacharjee, S., Scheelke, B., and Troutt, T. R., "Modification of Vortex Interactions in a Reattaching Separated Flow," *AIAA Journal*, Vol. 24, 1986, pp. 623–629.

[19]Zhang, Y. Q., Ho, C. M., and Monkewitz, P., "The Mixing Layer Forced by Fundamental and Subharmonic," *Laminar-Turbulent Transition*, edited by V. V. Kozlov, Springer-Verlag, 1985, pp. 385–396.

[20]Monkewitz, P. A., "Subharmonic Resonance, Pairing and Shredding in the Mixing Layer," *Journal of Fluid Mechanics*, Vol. 188, 1988, pp. 223–252.

[21]Raman, G., and Rice, E. J., "Subharmonic and Fundamental High Amplitude Excitation of an Axisymmetric Jet," AIAA Paper 89-0993, 1989.

[22]Ng, T. T., and Bradley, T. A., "Effect of Multi-frequency Forcing on the Near Field Development of a Jet," AIAA Paper 87-0054, 1987.

[23]Kibens, V., "Discrete Noise Spectrum Generated by an Acoustically Excited Jet," *AIAA Journal*, Vol. 18, 1980, pp. 434–441.

[24]Fiedler, H. E., and Mensing, P., "The Plane Turbulent Shear Layer with Periodic Excitation," *Journal of Fluid Mechanics*, Vol. 150, 1985, pp. 281–309.